

See discussions, stats, and author profiles for this publication at: <https://www.researchgate.net/publication/268792640>

Metal–Organic Framework Derived Magnetic Nanoporous Carbon: Novel Adsorbent for Magnetic Solid–Phase Extraction

ARTICLE in ANALYTICAL CHEMISTRY · NOVEMBER 2014

Impact Factor: 5.64 · DOI: 10.1021/ac5031896 · Source: PubMed

CITATIONS

6

READS

49

6 AUTHORS, INCLUDING:



Chun Wang

Agricultural University Of Hebei

160 PUBLICATIONS 2,403 CITATIONS

[SEE PROFILE](#)



Qiuhua Wu

85 PUBLICATIONS 1,710 CITATIONS

[SEE PROFILE](#)



Zhi Wang

Sun Yat-Sen University

188 PUBLICATIONS 1,277 CITATIONS

[SEE PROFILE](#)

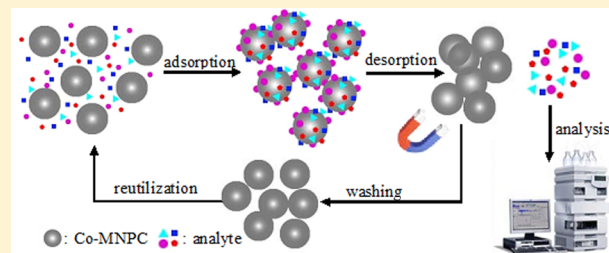
Metal–Organic Framework Derived Magnetic Nanoporous Carbon: Novel Adsorbent for Magnetic Solid-Phase Extraction

Lin Hao, Chun Wang, Qiuhsua Wu, Zhi Li, Xiaohuan Zang, and Zhi Wang*

Department of Chemistry, College of Science, Agricultural University of Hebei, Baoding 071001, China

Supporting Information

ABSTRACT: The fabrication of a magnetic nanoporous carbon (MNPC) via one-step direct carbonization of Co-based metal–organic framework has been achieved without using any additional carbon precursors. The morphology, structure, and magnetic behavior of the as-prepared Co-MNPC were characterized by using the techniques of scanning electron microscopy, transmission electron microscopy, powder X-ray diffraction, Raman spectroscopy, N₂ adsorption, and vibrating sample magnetometer. The Co-MNPC has a high specific surface area, large pore volume, and super paramagnetism. Its performance was evaluated by the magnetic solid-phase extraction of some neonicotinoid insecticides from water and fatmelon samples followed by high-performance liquid chromatographic analysis. The effects of the main experimental parameters that could affect the extraction efficiencies were investigated. The results demonstrated that the Co-MNPC had an excellent adsorption capability for the compounds.



Sample preparation is considered as the most critical step in an overall analytical process since it has a multifarious role related to the extraction, preconcentration, and cleanup of the analytes from the coexisting species in the sample.¹ Recently, a new mode of solid-phase extraction (SPE), which was based on the use of magnetic or magnetically modified adsorbents called magnetic solid-phase extraction (MSPE), has been developed.² In MSPE, the phase separation of the solid magnetic absorbent from a liquid sample can be conducted directly by using an external magnet without the need of additional filtration or centrifugation procedures, which makes the separation faster and easier. Besides, MSPE can avoid the time-consuming column passing operations encountered in common SPE. Due to the key role of the MSPE adsorbent materials in MSPE, the exploration of new types of MSPE adsorbents to improve the extraction efficiency for different kinds of analytes has become an active research field in analytical chemistry.³ Since carbon materials often exhibit a high adsorption capacity for organic compounds, magnetic carbon materials, such as magnetic carbon nanotubes, graphene, and carbon nanofibers, have been dominantly explored as the MSPE adsorbents for trapping or separation of some organic compounds.^{4,5}

Nanoporous carbons (NPCs), with their advantageous characteristics of having lightweight, good electron mobility, high thermal conductivity, extraordinary elasticity, stiffness, fast kinetics, and high surface area, have been considered as the promising materials for use in gas adsorption, electrochemical capacitance, sensing, and catalysis.^{6–8} Several methods have been employed to prepare NPCs, such as laser ablation, chemical vapor decomposition (CVD), electrical arc, and nanocasting, as well as chemical or physical activation methods.⁹ Among these methods, the nanocasting method is

an effective way to prepare microporous and mesoporous carbon materials.^{10,11} So far, many traditional inorganic porous materials, such as ordered mesoporous silica (e.g., MCM-48, SBA-1, SBA-15, SBA-16, HMS),^{12,13} and zeolites,¹⁴ have been successfully used as the hard templates for the preparation of nanoporous carbons by using the nanocasting method. However, this strategy was also somewhat time-consuming and costly since it involved complicated multistep synthetic procedures, which made it unfavorable for large-scale preparations.^{15,16}

More recently, metal–organic frameworks (MOFs) have received great interest as a novel class of crystalline nanoporous materials.¹⁷ MOFs, with their fascinating diverse structures, permanent nanoscale porosities, high surface area, and uniform structured cavities,¹⁸ have been demonstrated to be ideal templates for fabricating nanoporous carbons.¹⁷ So far, several MOFs, such as MOF-5, ZIF-8, Fe-MOF, and Al-PCP, have been proven to be promising precursors for yielding MOFs-derived nanoporous carbons.^{10,19–21} Such NPCs have shown excellent properties in the use for electrochemical capacitance,^{22,23} gas adsorption,²⁴ and catalysis.²⁵ However, the potential applications of such nanoporous carbon materials as the adsorbents in sample preparations have not yet been explored. Co-based MOF (ZIF-67), which was formed by bridging 2-methylimidazolate anions and cobalt cations, had a sodalite topology.²⁶ It was promising for the selective capture of CO₂ and also for other potential applications in separation and

Received: August 25, 2014

Accepted: November 20, 2014

Published: November 20, 2014



catalysis.²⁷ ZIF-67 might be used as a potential precursor for the preparation of a NPC.

In this study, a novel Co-based magnetic nanoporous carbon (Co-MNPC) was fabricated by one-step direct carbonization of ZIF-67 without using any additional carbon precursors. The so-prepared Co-MNPC not only possesses high specific surface area but also has a strong magnetism due to the formation of Co nanoparticles in the carbonization process. It has been reported that neonicotinoid insecticide residues can enter the human system through the direct consumption of the contaminated food or through the food products obtained from the animals that were fed with the contaminated feed and fodder.²⁸ This may pose a potential hazard to both human health and ecosystem. To evaluate the performance of the Co-MNPC in MSPE, several neonicotinoid insecticides, which have been most commonly used on rice, rape, potatoes, vegetables, and fruits crops in local areas, were selected as the model analytes. As a result, an effective MSPE method for the extraction of the neonicotinoid insecticides from water and fatmelon samples was established prior to their determination by high-performance liquid chromatography-ultraviolet detection (HPLC-UV).

EXPERIMENTAL SECTION

Reagents and Materials. Acetonitrile (HPLC-grade) was purchased from Sinopharm Chemical Reagent Co. (Beijing, China). $\text{Co}(\text{NO}_3)_2 \cdot 6\text{H}_2\text{O}$, 2-methylimidazole, methanol, acetone, hydrochloric acid (HCl), sodium hydroxide (NaOH), and all the other reagents were purchased from Beijing Chemical Reagents Company (Beijing, China). The water used throughout the work was double-distilled on a SZ-93 automatic double-distiller purchased from Shanghai Yarong Biochemistry Instrumental Factory (Shanghai, China). Imidacloprid (ICL), acetamiprid (ACT), thiacloprid (TCL), and thiamethoxam (TMX) were purchased from Agricultural Environmental Protection Institution (Tianjin, China). A mixture stock solution containing TMX, ICL, ACT, and TCL each at $20.0 \mu\text{g mL}^{-1}$ was prepared in methanol. A series of standard solutions were prepared by mixing an appropriate amount of the stock solution with methanol in a 10 mL volumetric flask. All the standard solutions were stored at 4°C in the dark.

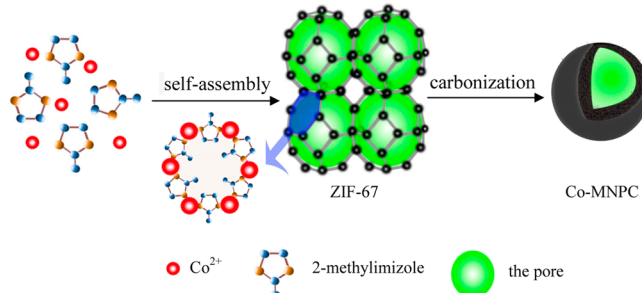
Instruments. An Agilent Technologies 1260 Infinity LC with G1314F 1260 VWD detector was used for all the experiments. A Centurysil C18 column ($250 \times 4.6 \text{ mm id}, 5.0 \mu\text{m}$) from Dalian Johnsson Separation Science Technology Corporation (Dalian, China) was used for separations. The mobile phase was a mixture of acetonitrile-water (20:80 v/v) at a flow rate of 1.0 mL min^{-1} . The UV monitoring wavelengths were chosen at 253, 270, 244, and 244 nm for TMX, ICL, ACT, and TCL, respectively.

Scanning electron microscopy (SEM) images were conducted by a S-4300 SEM instrument (HITACHI, Japan). Transmission electron microscopy (TEM) was observed by a JEOL model JEM-2011(HR) (Tokyo, Japan). X-ray diffraction (XRD) measurements were made with Cu K α radiation on a Brooker D8 ADVANC (Germany). The energy dispersive X-ray spectroscopy (EDS) spectra were taken on a TEAM energy spectrometer (EDAX USA). Raman spectroscopy (LavRAM Aramis, HORIBA Jobin Yvon, France) was conducted with a 532 nm laser to analyze the surface chemical structures of the products. The Brunauer–Emmett–Teller (BET) surface areas were determined from the N_2 adsorption at 300 K using a V-Sorb 2800P (Jinaipu, China). The magnetic property was

analyzed using a MPMS-XL-7 vibrating sample magnetometer (VSM) (Quantum Design) at room temperature.

Synthesis of Co-MNPC. ZIF-67 was prepared via a simple precipitation reaction in aqueous solution at room temperature according to a previous report.²⁹ Typically, a 20 mL aqueous solution of 2-methylimidazole (0.45 g, 5.48 mmol) with a 3 mL aqueous solution of $\text{Co}(\text{NO}_3)_2 \cdot 6\text{H}_2\text{O}$ (0.45 g, 1.55 mmol) was mixed, and then the mixture was stirred at room temperature for 6 h. The resulting purple precipitate was collected by centrifugation, washed with methanol 3 times, and finally dried at 80°C for 24 h. The carbonization of the ZIF-67 was performed at 700°C for 6 h under a nitrogen flow. The overall preparation process is illustrated in Scheme 1.

Scheme 1. Schematic Illustration of the Synthetic Process of Co-MNPC



Sample Preparation. Water samples were filtered through a 0.45 mm filter prior to MSPE extraction. Fresh fatmelon samples were cut into small pieces and homogenized in a laboratory homogenizer. A 200.0 g portion of the homogenized fatmelon sample was accurately weighed and then placed in a screw-capped glass test tube with a conical bottom. The samples were centrifuged at 4000 rpm for 10 min. Then, the sedimented phase was washed with 100 mL of double-distilled water. All the supernatants were combined together to a 500 mL volumetric flask to which double-distilled water was added to complete the volume. The sample solution was stored at 4°C for the subsequent MSPE extractions.

MSPE Procedures. For the MSPE of the neonicotinoid insecticides, 10.0 mg of the Co-MNPC was added to 50 mL sample solution in a conical flask. The mixture was shaken on a slow-moving platform shaker for 20 min. Next, the Co-MNPC was separated from the aqueous phase using a magnet, and the resultant supernatant was discarded. Then, the Co-MNPC and the residual solution were all transferred to a 10 mL centrifuge tube. The Co-MNPC was aggregated again by placing a magnet to the outside of the tube wall so that the residual supernatant could be completely removed by a pipet. Finally, 0.2 mL acetone was added into the isolated Co-MNPC and vortexed for 1 min to desorb the analytes. This desorption operation was repeated one more time. The desorption solutions were combined together and transferred to a 2 mL microcentrifuge tube. Finally $20.0 \mu\text{L}$ of the desorption solution was injected into the HPLC system for analysis.

Prior to next use, the used Co-MNPC nanoparticles were washed three times with 1 mL of acetone and then with 1 mL of water by vortexing for 1 min, respectively.

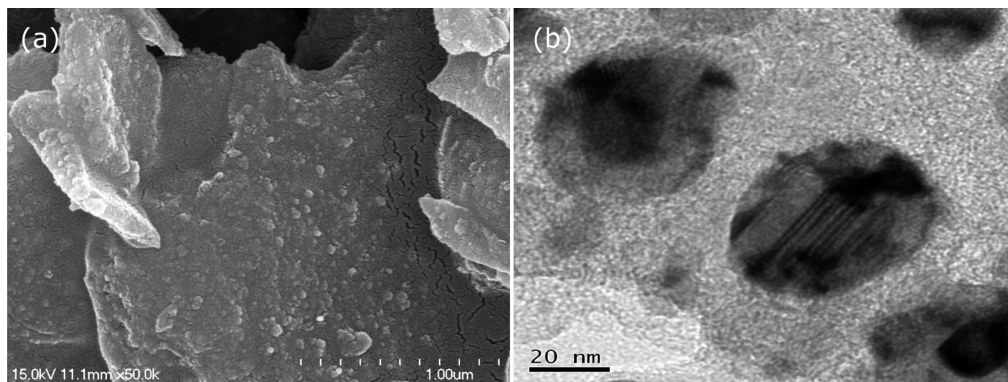


Figure 1. (a) SEM and (b) TEM images of the Co-MNPC.

RESULTS AND DISCUSSION

Synthesis and Characterization of the Co-MNPC. In this study, the Co-MNPC was fabricated by one-step direct carbonization of ZIF-67 without using any other additional carbon precursors. First, the carbonization temperature of the ZIF-67 was evaluated by carrying out the carbonization experiment at 500, 600, 700, and 800 °C for 6 h under a nitrogen flow, respectively. It was found that when the carbonization temperature was 500 or 600 °C, the carbonization of the ZIF-67 was insufficient, and the magnetism of the MNPC was weak; when the carbonization temperature was 700 °C, ZIF-67 could be fully carbonated and the magnetism of the MNPC was sufficient for the MSPE. However, when the carbonization temperature was further increased to 800 °C, the adsorption capacity of the resulting MNPC obviously declined. The reason for this may be because the original crystal shape of the ZIF-67 was collapsed after the carbonization at too high of a temperature. Next, different carbonization times (4, 5, 6, and 7 h) for the ZIF-67 were investigated. As a result, when the carbonization time was 4 h, the ZIF-67 could not be well-carbonated; when the carbonization time exceeded 5 h, the ZIF-67 could be completely carbonated. Finally, the carbonization for the ZIF-67 was chosen at 700 °C for 6 h. In addition, the reproducibility of the formation of the Co-MNPC from ZIF-67 was investigated by comparing the adsorption capacity of the resulting Co-MNPC prepared in different batches for the analytes. Experimental results showed that the adsorption capacity of the Co-MNPC for the analytes has no obvious changes with a relative standard deviation (RSD) of 5.5% from batch-to-batch.

To observe the morphology of the MNPC, SEM and TEM images were taken for the Co-MNPC. The SEM image of the composite (Figure 1a) shows a porous nature of the resulting carbon material, and the TEM image (Figure 1b) gives further evidence of its porous structure. The characterization of the MNPC was further investigated using XRD, EDS, and Raman spectroscopy. Figure S1 of the Supporting Information shows the characteristic XRD pattern of the Co-MNPC. The broad peak around $2\theta = 24^\circ$ in the XRD pattern of the Co-MNPC results mainly from the amorphous carbon of the Co-MNPC. This signal corresponds to the (002) spacing of the graphite, indicating that the carbon material has a typical graphite structure. The diffraction peaks of the composite at $2\theta = 44^\circ$ and 47° correspond to the metal cobalt and cobalt monoxide (JCPDS card no. 05-0727). On the other hand, C, O, and Co in the carbon material could be directly visualized from the EDS pattern in Figure S2 of the Supporting Information. As

illustrated in Figure S3 of the Supporting Information, the Raman spectra of the Co-MNPC display the two apparent bands at 1351 and 1592 cm^{-1} , respectively, which could be assigned to the typical D and G bands of the amorphous carbon. The G band is assigned to the vibration of all sp^2 hybridized carbon atoms of the carbon layers, while the D band is related to the disordered structure or graphene edges. The five bands at 191.3, 470.4, 512.3, 603.7, and 671.6 cm^{-1} can confirm the existence of Co_3O_4 in the MNPC.

The microporous characteristic and the macroscopic morphology of the Co-MNPC were analyzed via N_2 adsorption–desorption isotherms (Figure 2). It was deter-

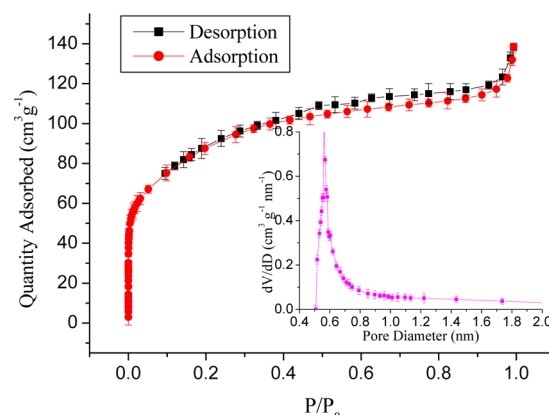


Figure 2. N_2 adsorption–desorption isotherms of the Co-MNPC.

mined that the Saito-Foley median pore width, total adsorption average pore width, total pore volume, and the experimental multipoint BET surface area of the Co-MNPC were 0.56 nm, 2.72 nm, $0.21 \text{ cm}^3 \text{ g}^{-1}$, and $314.50 \text{ m}^2 \text{ g}^{-1}$, respectively.

The VSM magnetization curves of the Co-MNPC obtained at 298 K are shown in Figure 3. It exhibits a typical super paramagnetic behavior. The saturation magnetization intensity of the Co-MNPC was 17.42 emu g^{-1} , which is sufficient for its magnetic separation from a solution with a strong magnet.

Optimization of the Experimental Conditions for the MSPE of the Neonicotinoid Insecticides by the Co-MNPC. The pores of the Co-MNPC with dimensions greater than 1 nm should be suitable for the adsorptions of some small organic molecules. Since the neonicotinoid insecticides are comparatively smaller molecules, they can be adsorbed into the pores of the Co-MNPC by simple π – π interactions and van der Waals' force. To evaluate the applicability of the Co-MNPC for

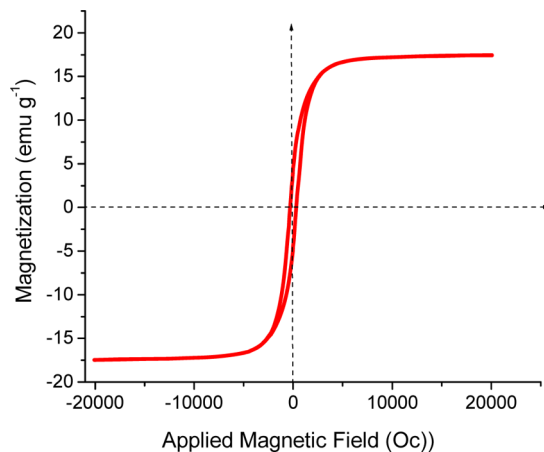


Figure 3. VSM magnetization curves of the Co-MNPC.

the extraction of the neonicotinoid insecticides from water and vegetable samples, the experimental parameters that might affect the performance of the extraction were investigated, including the amount of the Co-MNPC, extraction time, sample pH, ionic strength, and desorption conditions. All the experiments were performed in triplicate with a 50 mL water solution containing each of the neonicotinoids at 40 ng mL⁻¹ and the means of the results were used for optimization.

Amount of the Co-MNPC. In order to select the optimum dosage of the Co-MNPC for the extraction of the neonicotinoid insecticides, different amounts of the Co-MNPC were investigated in the range from 2 to 20 mg for the adsorption of the neonicotinoid insecticides. The result shows that the recovery could reach the maximum plateau when 7.5 mg of the magnetic sorbent was used. To ensure that the adsorbent was sufficient for the extraction, 10 mg of Co-MNPC was employed in the following experiment.

Extraction Time. The effect of extraction time on the extraction was conducted by changing the extraction time from 5 to 30 min. The experimental result showed that the extraction efficiency for the analytes was increased from 5 to 15 min and then remained almost unchanged. On the basis of the above result, 20 min of extraction time was chosen.

Salt Addition. Generally, the addition of salt to the sample has two functions. First, the addition of salt can decrease the solubility of the analytes in the sample solution due to salt-out effect, which is often favorable for the extraction. But on the other hand, it can also increase the viscosity of the solution, which is unfavorable for the extraction.³⁰ In this study, the effect of salt addition was studied by adding different amounts of sodium chloride [i.e., 0, 1.0, 2.0, 3.0, 5.0, and 10% (w/v)] to the sample solution. As a result, the extraction efficiencies for all of the neonicotinoid insecticides were almost independent of the addition of NaCl in the concentration range investigated. Therefore, no NaCl was added to the samples in all the subsequent experiments.

pH of Sample Solution. The pH of the sample solution is an important factor to affect the adsorption of the analytes since it can influence both the existing form and the stability of the analytes. In this study, the optimization of the pH of the sample solution was performed by changing the sample solution pH from 2 to 12. As shown in Figure 4a, there is maximum extraction efficiency for all of the analytes at about pH 6. The reason for this may be explained as follows: the analytes in the molecular form will be favorable for them to be

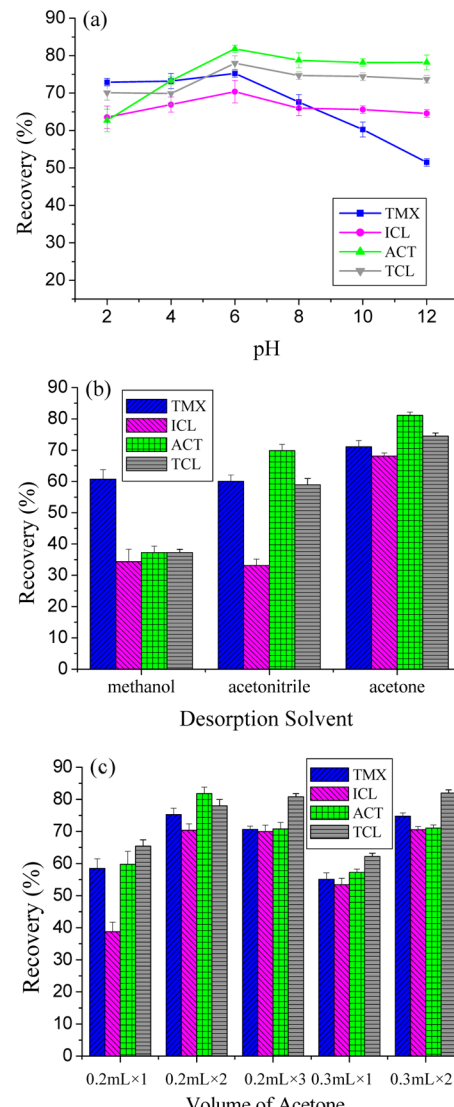


Figure 4. Effect of the experimental conditions on the extraction efficiency of the Co-MNPC for the neonicotinoid insecticides: (a) sample solution pH; (b) desorption solvents; and (c) the volume of acetone.

adsorbed on the adsorbent. When the pH of the sample solution was below 6.0, the analytes could be ionized and therefore their adsorption on the adsorbent would be weakened. When the sample solution pH exceeded 7, TMX could be broken down while the other analytes were relatively stable in the alkaline conditions. On the basis of the above experimental result, the pH of the sample solution was set at 6 for the experiment.

Desorption Conditions. To achieve an effective desorption of the analytes from the Co-MNPC, the most commonly used three organic solvent (i.e., acetonitrile, methanol, and acetone) were investigated as the desorption solvent. Figure 4b shows that acetone had a highest desorption efficiency for the analytes. The reason for this may be that acetone has a more similar polarity to the neonicotinoid insecticides and therefore has a relatively high dissolution capacity for the analytes. Therefore, acetone was chosen as the desorption solvent.

Then, the effect of the volume of acetone on the desorption was further investigated. It was shown that the simplest way for the effective desorption of the analytes from the sorbent could

Table 1. Analytical Performance Data for the Neonicotinoid Insecticides by the MSPE Method

analyte	water sample				fatmelon sample			
	linear range (ng mL ⁻¹)	r ²	RSD (%)	LOD (ng mL ⁻¹)	linear range (ng g ⁻¹)	r ²	RSD (%)	LOD (ng g ⁻¹)
TMX	0.05–50.0	0.9988	5.5	0.01	1.0–100.0	0.9984	5.3	0.20
ICL	0.10–50.0	0.9990	4.5	0.06	1.5–100.0	0.9980	6.8	0.50
ACT	0.05–50.0	0.9982	6.7	0.01	1.0–100.0	0.9987	5.3	0.20
TCL	0.10–50.0	0.9994	5.8	0.06	1.5–100.0	0.9994	4.8	0.50

Table 2. Analytical Results for the Determination of Neonicotinoid Insecticides in Water and Fatmelon Samples

analyte	river water				pond water				fatmelon sample		
	spiked (ng mL ⁻¹)	found (ng mL ⁻¹)	R ^b (%)	RSD (%)	found (ng mL ⁻¹)	R ^b (%)	RSD (%)	spiked (ng g ⁻¹)	found (ng g ⁻¹)	R ^b (%)	RSD (%)
TMX	0	0.04			nd ^a			0	0.65		
	5	4.99	99.0	5.9	4.8	96.0	5.9	5	5.32	93.4	5.5
	20	19.8	99.1	4.3	19.7	99.8	4.3	20	20.1	97.3	3.7
ICL	0	nd ^a			nd ^a			0	nd ^a		
	5	4.78	95.6	3.6	4.88	97.6	3.6	5	4.65	93.0	3.1
	20	19.6	98.0	4.4	19.3	96.5	4.4	20	19.8	99.3	4.5
ACT	0	nd ^a			nd ^a			0	0.74		
	5	4.88	97.6	4.1	4.82	96.4	4.1	5	5.46	94.4	4.9
	20	19.5	97.5	6.2	19.7	98.5	6.2	20	20.3	98.0	4.2
TCL	0	nd ^a			nd ^a			0	nd ^a		
	5	4.77	95.4	4.5	4.72	94.4	4.5	5	4.8	96.0	5.8
	20	19.45	97.2	5.2	19.67	98.4	5.2	20	19.5	97.5	3.4

^and: not detected. ^bR: recovery of the method.

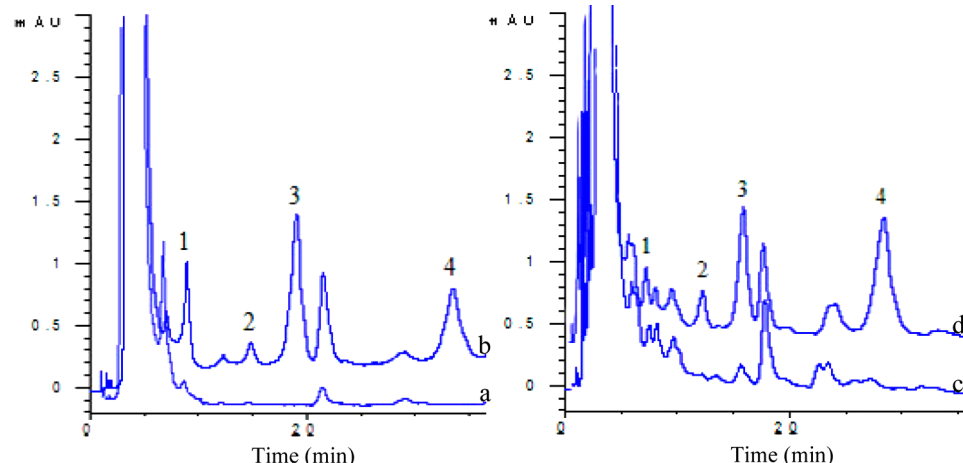


Figure 5. Typical chromatograms of (a) river water and the river water spiked with the neonicotinoid insecticides at each concentration of (b) 5.0 ng mL⁻¹; (c) fatmelon sample and the fatmelon sample spiked with the neonicotinoid insecticides at each concentration of (d) 10.0 ng g⁻¹. Peak identifications: 1. TMX, 2. ICL, 3. ACT, 4. TCL.

be achieved by eluting the sorbent with 0.2 mL acetone twice (0.2 mL × 2) (see Figure 4c). After the combination of the two desorption solutions, 20 μL was injected into the HPLC system for analysis.

Reusability of the Co-MNPC. After the desorption of the analytes from the adsorbent, prior to next use, the used Co-MNPC was washed three times with 1 mL of acetone and then with 1 mL of water by vortexing for 1 min. The experimental result showed that the Co-MNPC could be reused at least 15 times without a significant loss of its adsorption capacity.

Adsorption Kinetic Study. For the adsorption kinetic study of the Co-MNPC for the analytes, 50 mL solution containing 40 ng mL⁻¹ each of the neonicotinoid insecticides mixed with 10 mg of the Co-MNPC particles was used for the experiment and a pseudo-second-order model^{31,32} was assumed

for the adsorption process to fit the experimental data. The pseudo-second-order model can be expressed as the following equation:

$$\frac{t}{q_t} = \frac{1}{kq_e^2} + \frac{1}{q_e}$$

Where q_e and q_t (mg g⁻¹) represent the amounts of the adsorbed analytes at equilibrium and at a time t (min), respectively, and k (g mg⁻¹ min⁻¹) is the adsorption rate constant. The k and q_e could be determined from the intercept and slope of the plot obtained by plotting t/q_t versus t. The experimental result showed a good linear relationship between t/q_t and t with the correlation coefficient (r²) larger than 0.9990, which confirmed the applicability of the pseudo-

Table 3. Comparison of the Current Method with other Relevant Reported Methods

method	sample	linearity	LODs	RSDs (%)	ref
SPE-HPLC-DAD ^a	bovin milk	—	3–10 (ng g ⁻¹)	2.5–6.8	28
SPE-HPLC-MS/MS ^b	chestnut, shallot	4–100 (ng mL ⁻¹)	10–100 (ng g ⁻¹)	5.1–8.6	33
DSPE ^c -HPLC-DAD	rice, maize	20–450 (ng g ⁻¹)	2–5 (ng g ⁻¹)	0.9–12.6	34
LLME ^d -HPLC-MS/MS	honey	1.5–100 (ng g ⁻¹)	5–10 (ng g ⁻¹)	0.6–16	35
DLLME-MEKC ^e	cucumber	2.7–200 (ng g ⁻¹)	0.8–1.2 (ng g ⁻¹)	3.8–4.4	36
MSPE-HPLC-DAD	pear and tomato	0.5–100 (ng g ⁻¹)	0.08–0.15 (ng g ⁻¹)	2.4–6.3	37
MSPE-HPLC-UV	lemon juice	0.3–100 (ng mL ⁻¹)	0.08–0.2 (ng mL ⁻¹)	4.6–7.1	38
MSPE-HPLC-UV	water	0.01–50.0 (ng mL ⁻¹)	0.01–0.04 (ng mL ⁻¹)	4.5–6.7	this work
	fatmelon sample	1.0–100.0 (ng g ⁻¹)	0.2–0.5 (ng g ⁻¹)	5.3–6.8	

^aDAD: diode array detection. ^bMS/MS: tandem mass spectrometry. ^cDSPE: dispersive solid-phase extraction. ^dLLME: liquid–liquid microextraction. ^eDLLME-MEKC: dispersive liquid–liquid microextraction-micellar electrokinetic chromatography.

second-order equation to the current adsorption process. In addition, the calculated q_e values from the pseudo-second order model agreed well with the experimental data (see Table S1 of the Supporting Information). On the basis of the assumption of the pseudo-second-order model,^{31,32} these experimental results indicated that the adsorption of the neonicotinoid insecticides on the Co-MNPC are mainly due to a chemical adsorption.

Quantitative Analysis. The calibration curves, limits of detection (LODs), correlation coefficients (r^2), and the repeatability were studied under the above-optimized conditions for the analysis of the neonicotinoid insecticides. The results are summarized in Table 1.

The calibration curves for the analytes were established for water and fatmelon samples by the peak areas of the analytes versus their corresponding concentrations with a linear least-squares regression analysis. As a result, for the water sample, the linearity for all the analytes existed in the concentration range of 0.05–50.0 ng mL⁻¹ with the correlation coefficients (r^2) ranging from 0.9982 to 0.9994; for fatmelon sample, a good linearity for the analytes was observed in the concentration range of 1.0–100.0 ng g⁻¹ with the correlation coefficients (r^2) between 0.9980 and 0.9994. The LODs, calculated as the corresponding concentrations at which the signal-to-noise ratios were equal to 3, were in the range from 0.01 to 0.06 ng mL⁻¹ for the water sample and from 0.2 to 0.5 ng g⁻¹ for the fatmelon sample.

Real Samples Analysis. The optimized MSPE method with the Co-MNPC as the adsorbent was used for the extraction of neonicotinoid insecticides both from river water, pond water samples, and from the fatmelon sample bought from a local market in Baoding (China). The results are shown in Table 2. As a result, the river water was found to contain 0.04 ng mL⁻¹ of TMX, and the fatmelon sample was found to be contaminated by TMX at 0.65 ng g⁻¹ and by ACT at 0.74 ng g⁻¹, respectively; none of the neonicotinoid insecticides were found in pond water. The determined recoveries of the method for the analytes were in the range from 93.0% to 99.8% with RSDs between 3.1% and 6.2%. Figure 5 shows the typical chromatograms of the river water and fatmelon samples before and after being spiked with each of the neonicotinoid insecticides.

Comparison of the MSPE Method with Other Reported Methods. For the evaluation of the current method, it was compared with the other reported methods in the literature for the determination of neonicotinoid insecticides from the viewpoint of linear range, LODs, and RSDs. The comparison results are shown in Table 3. The data in Table 3 illustrate that the current method has comparable

linear ranges and RSDs with the other reported methods and also the sensitivity of the current method is better than or comparable with that obtained with the reported SPE,^{28,33,34} LLME,^{35,36} or MSPE^{37,38} methods. Compared with traditional adsorbents, the magnetic adsorbent can make the phase separation process easier and faster during the extraction without the need for additional centrifugation or filtration procedures and MSPE can also avoid the time-consuming column passing operations encountered in common SPE. Also, another main advantage of the current method is that it only involves the use of the HPLC-UV instrument, which is currently available to virtually all analytical laboratories.

CONCLUSIONS

In conclusion, a magnetic nanoporous carbon, Co-MNPC, was fabricated by a one-step direct carbonization of ZIF-67 without using any other additional carbon precursors. The prepared nanocomposite had a high surface area, super magnetism, and good adsorption performance. It was used as the MSPE adsorbent to extract and concentrate some neonicotinoid insecticides from water and fatmelon samples. A wide linear range, low LODs, and good recoveries of the method for the analytes indicated that the Co-MNPC MSPE method can satisfy the determination of the studied analytes in real samples. This study opens up a new way for the development of new types of magnetic nanoporous carbon materials of high adsorption capacity for the application in MSPE.

ASSOCIATED CONTENT

S Supporting Information

Adsorption kinetic parameters of the neonicotinoid insecticides on the Co-MNPC; XRD pattern of the Co-MNPC; EDS analysis of the Co-MNPC; and Raman spectra of the Co-MNPC. This material is available free of charge via the Internet at <http://pubs.acs.org>.

AUTHOR INFORMATION

Corresponding Author

*E-mail: zhiwang2013@aliyun.com and wangzhi@hebau.edu.cn. Tel: +86 312 7521513. Fax: +86 312 7521513.

Notes

The authors declare no competing financial interest.

ACKNOWLEDGMENTS

Financial supports from the National Natural Science Foundation of China (Grants 31171698 and 31471643), the Innovation Research Program of the Department of Education

of Hebei for Hebei Provincial Universities (Grant LJRC009), the Natural Science Foundations of Hebei (Grant B2012204028), and the Scientific and Technological Research Foundation of the Department of Education of Hebei Province (Grant ZD20131033) are gratefully acknowledged.

■ REFERENCES

- (1) Giokas, D. L.; Zhu, Q.; Pan, Q.; Chisvert, A. *J. Chromatogr. A* **2012**, *1251*, 33–39.
- (2) Chen, L.; Wang, T.; Tong, J. *TrAC, Trends Anal. Chem.* **2011**, *30*, 1095–1108.
- (3) Huo, S.-H.; Yan, X.-P. *Analyst* **2012**, *137*, 3445.
- (4) Xie, L.; Jiang, R.; Zhu, F.; Liu, H.; Ouyang, G. *Anal. Bioanal. Chem.* **2014**, *406*, 377–399.
- (5) Scida, K.; Stege, P. W.; Haby, G.; Messina, G. A.; García, C. D. *Anal. Chim. Acta* **2011**, *691*, 6–17.
- (6) Yang, S. J.; Kim, T.; Im, J. H.; Kim, Y. S.; Lee, K.; Jung, H.; Park, C. R. *Chem. Mater.* **2012**, *24*, 464–470.
- (7) Vinu, A.; Hossian, K. Z.; Srinivasu, P.; Miyahara, M.; Anandan, S.; Gokulakrishnan, N.; Mori, T.; Ariga, K.; Balasubramanian, V. V. *J. Mater. Chem.* **2007**, *17*, 1819–1825.
- (8) Li, Q.; Jiang, R.; Dou, Y.; Wu, Z.; Huang, T.; Feng, D.; Yang, J.; Yu, A.; Zhao, D. *Carbon* **2011**, *49*, 1248–1257.
- (9) Hu, M.; Reboul, J.; Furukawa, S.; Torad, N. L.; Ji, Q.; Srinivasu, P.; Ariga, K.; Kitagawa, S.; Yamauchi, Y. *J. Am. Chem. Soc.* **2012**, *134*, 2864–2867.
- (10) Radhakrishnan, L.; Reboul, J.; Furukawa, S.; Srinivasu, P.; Kitagawa, S.; Yamauchi, Y. *Chem. Mater.* **2011**, *23*, 1225–1231.
- (11) Wang, X.; Bozhilov, K. N.; Feng, P. *Chem. Mater.* **2006**, *18*, 6373–6381.
- (12) Tang, Z.-h.; He, X.; Song, Y.; Liu, L.; Guo, Q.-g.; Yang, J.-h. *New Carbon Materials* **2010**, *25*, 465–469.
- (13) Momčilović, M. Z.; Randelović, M. S.; Zarubica, A. R.; Onjia, A. E.; Kokunešoski, M.; Matović, B. Z. *Chem. Eng. J.* **2013**, *220*, 276–283.
- (14) Kyotani, T.; Ma, Z.; Tomita, A. *Carbon* **2003**, *41*, 1451–1459.
- (15) Huang, Y.; Cai, H.; Feng, D.; Gu, D.; Deng, Y.; Tu, B.; Wang, H.; Webley, P. A.; Zhao, D. *Chem. Commun.* **2008**, 2641–2643.
- (16) Yang, S. J.; Kim, T.; Lee, K.; Kim, Y. S.; Yoon, J.; Park, C. R. *Carbon* **2014**, *71*, 294–302.
- (17) Chaikittisilp, W.; Ariga, K.; Yamauchi, Y. *J. Mater. Chem. A* **2013**, *1*, 14–19.
- (18) Gu, Z.-Y.; Yang, C.-X.; Chang, N.; Yan, X.-P. *Acc. Chem. Res.* **2012**, *45*, 734–745.
- (19) Jiang, H. L.; Liu, B.; Lan, Y. Q.; Kuratani, K.; Akita, T.; Shioyama, H.; Zong, F.; Xu, Q. *J. Am. Chem. Soc.* **2011**, *133*, 11854–11857.
- (20) Banerjee, A.; Gokhale, R.; Bhatnagar, S.; Jog, J.; Bhardwaj, M.; Lefez, B.; Hannoyer, B.; Ogale, S. *J. Mater. Chem.* **2012**, *22*, 19694–19699.
- (21) Li, J. S.; Li, S. L.; Tang, Y. J.; Li, K.; Zhou, L.; Kong, N.; Lan, Y. Q.; Bao, J. C.; Dai, Z. H. *Sci. Rep.* **2014**, *4*, 5130–5137.
- (22) Xu, G.; Ding, B.; Shen, L.; Nie, P.; Han, J.; Zhang, X. *J. Mater. Chem. A* **2013**, *1*, 4490–4496.
- (23) Hu, J.; Wang, H.; Gao, Q.; Guo, H. *Carbon* **2010**, *48*, 3599–3606.
- (24) Shahid, S.; Nijmeijer, K. *J. Membr. Sci.* **2014**, *459*, 33–44.
- (25) Kim, J.; McNamara, N. D.; Her, T. H.; Hicks, J. C. *ACS Appl. Mater. Interfaces* **2013**, *5*, 11479–11487.
- (26) Qian, J.; Sun, F.; Qin, L. *Mater. Lett.* **2012**, *82*, 220–223.
- (27) Yang, H.; He, X.-W.; Wang, F.; Kang, Y.; Zhang, J. *J. Mater. Chem.* **2012**, *22*, 21849–21851.
- (28) Seccia, S.; Fidente, P.; Montesano, D.; Morrica, P. *J. Chromatogr. A* **2008**, *1214*, 115–120.
- (29) Torad, N. L.; Hu, M.; Ishihara, S.; Sukegawa, H.; Belik, A. A.; Imura, M.; Ariga, K.; Sakka, Y.; Yamauchi, Y. *Small* **2014**, *10*, 2096–2107.
- (30) Liu, L.; Feng, T.; Wang, C.; Wu, Q.; Wang, Z. *J. Sep. Sci.* **2014**, *37*, 1276–1282.
- (31) Ho, Y.-S.; McKay, G. *Process Biochem.* **1999**, *34*, 451–465.
- (32) Vadivelan, V.; Kumar, K. V. *J. Colloid Interface Sci.* **2005**, *286*, 90–100.
- (33) Xie, W.; Han, C.; Qian, Y.; Ding, H.; Chen, X.; Xi, J. *J. Chromatogr. A* **2011**, *1218*, 4426–4433.
- (34) Wang, P.; Yang, X.; Wang, J.; Cui, J.; Dong, A. J.; Zhao, H. T.; Zhang, L. W.; Wang, Z. Y.; Xu, R. B.; Li, W. J.; Zhang, Y. C.; Zhang, H.; Jing, J. *Food Chem.* **2012**, *134*, 1691–1698.
- (35) Jovanov, P.; Guzsvány, V.; Franko, M.; Lazic, S.; Sakac, M.; Saric, B.; Banjac, V. *Talanta* **2013**, *111*, 125–133.
- (36) Zhang, S.; Yang, X.; Yin, X.; Wang, C.; Wang, Z. *Food Chem.* **2012**, *133*, 544–550.
- (37) Ma, X.; Wang, J.; Sun, M.; Wang, W.; Wu, Q.; Wang, C.; Wang, Z. *Anal. Methods* **2013**, *5*, 2809–2815.
- (38) Liu, L.; Feng, T.; Wang, C.; Wu, Q.; Wang, Z. *J. Sep. Sci.* **2014**, *37*, 1276–1282.